# Study of the structure factor anisotropy and long range correlations of ferrofluids in the dilute low-coupling regime

Juan J. Cerdà [a,b,*], Ekaterina Elfimova [c], V. Ballenegger [d], Ekaterina Krutikova [c], Alexey Ivanov [c], Christian Holm [b]

[a] Instituto de Física Interdisciplinar y Sistemas Complejos IFISC (CSIC-UIB), Universitat de les Illes Balears, 07122 Palma de Mallorca, Spain
[b] Institute for Computational Physics, Pfaffenwaldring 27, Universität Stuttgart, 70569 Stuttgart, Germany
[c] Department of Mathematical Physics, The Urals State University, 51 Lenin Avenue, Ekaterinburg 620083, Russia
[d] Institut UTINAM, Université de Franche-Comté, Route de Gray 16, 25030 Besancon, France

## ARTICLE INFO

## ABSTRACT

Dipolar soft-sphere (DSS) fluids in the dilute low-coupling regime are studied via Molecular Dynamic simulations and the extension of a theoretical formalism previously used for dipolar hard spheres in which new terms for the virial expansion of the radial distribution function corresponding to the three-particle contribution are presented and tested for the zero and non-zero magnetic field case. A thorough comparison with simulations shows that the extended formalism is able to account for the structure factors of DSS with and without externally applied magnetic fields in the dilute low-coupling regime: quantitative agreement between theory and simulations is found for dipolar coupling parameters $\lambda \lesssim 2$, and volume fraction $\varphi \lesssim 0.25$. When $\lambda > 1$ the new added term to the virial expansion is observed to play a crucial role in order to match quantitatively theory and simulations at zero field. In the presence of an external magnetic field our tests show that further improvements are needed and only new terms with Langevin function dependences can significantly contribute to improve the predictions for the dilute low-coupling regime. Numerical simulations show that despite that the ferrofluids considered here are in the dilute low-coupling regime, when an external field is applied, important correlations along the parallel direction to the field and depletion phenomena along the perpendicular direction are observed in the averaged density surrounding a particle.

© 2010 Elsevier B.V. All rights reserved.

## 1. Introduction

Ferrofluids are colloidal suspensions of monodomain ferromagnetic nanoparticles stabilized against aggregation by steric coatings (in non-electrolyte solutions) or by electrical double layers (in aqueous solutions). Despite the differences in sizes and magnetic materials that can be used to make ferrofluid particles [1,2], the behavior of a monodisperse ferrofluid system can be characterized by two dimensionless parameters: the volume fraction of particles $\varphi = N v_p / V$ (where $N$ is the number of particles, $v_p$ is the volume of a particle and $V$ the total volume of the system), and the dipolar coupling parameter $\lambda = 0.5 U_{dd}/k_B T$, where $U_{dd}$ is the interaction energy of two particles in head-to-tail contact. Typical ferrofluids have a volume fraction of suspended magnetic material about 7% in volume, raising to a 23% when their surfactant is included [3]. The value of $\lambda$ strongly depends on the material and size [2]:

conventional maghemite ($\gamma-Fe_2O_3$) or magnetite ($Fe_3O_4$) ferrofluids with particle size 5–10 nm have a value of $\lambda < 1$, $\varepsilon-Co$ particles and iron ($Fe_{0.75}Co_{0.25}$) dispersions have been reported to have typical values of $\lambda \approx 2.5$. More recently magnetite and Co particles of larger size with $\lambda$ up to 7 and 14, respectively, has been synthesized [2]. Magnetite colloids extracted from magnetotactic bacteria have been reported to have even larger dipole strengths ($\lambda \approx 70$) [2]. When a uniform stationary magnetic field $\boldsymbol{H}$ is introduced, a third dimensionless parameter, the Langevin parameter $\alpha \equiv \mu H/(k_B T)$ (where $\mu$ is the typical magnetic dipole of the particles) is needed to characterize the system. The use of $\varphi$, $\lambda$ and $\alpha$ allows a generalized description of ferrofluid systems.

In the non-aggregating regime $\lambda < 2$, the physical properties of very dilute systems ($\varphi \to 0$) are well described using the framework of the one-particle model [4], which treats the ferrofluid as an ideal paramagnetic gas of particles suspended in a liquid carrier. However, this model breaks down when either the particle concentration or the strength of the dipole–dipole interaction are increased. Although in this regime the number of aggregates is negligible, correlations among particles exist. Several theoretical models have been proposed in order to explain the magnetic properties of ferrofluids in this

* Corresponding author at: Instituto de Física Interdisciplinar y Sistemas Complejos IFISC (CSIC-UIB), Universitat de les Illes Balears, 07122 Palma de Mallorca, Spain. Tel.: +34 971 259906; fax: +34 971 173248.
E-mail address: joan@ifisc.uib-csic.es (J.J. Cerdà).

regime which are based on adapted versions of the mean-field [5,6], and mean-spherical [7–12] models, as well as the thermodynamic perturbation model [13,14]. In the non-aggregating regime, structure factors determined experimentally are a valuable source of information [15–18], but it is difficult to extract from them a detailed knowledge about the correlations of the ferrofluid particles. Thus, theoretical methods that can relate the observed structure factors to the interparticle correlations in the ferrofluid are desirable. In order to get insight about the observed radial distribution functions and structure factors a theoretical framework has been recently proposed [19] for the case of dipolar hard spheres (DHS) at zero-field in the low-coupling regime $\lambda < 2$. However, that model has not been stringently tested against numerical results.

In this work we aim to study in depth the low-coupling regime via a combination of numerical simulations and an extension of the theoretical formalism of Elfimova et al. [19] to the case of dipolar soft-spheres (DSS) at zero and non-zero field. The soft-core interaction here considered is a cut-shifted Lennard-Jones potential, also called Weeks–Chander–Andersen (WCA) potential [20], of the form

$$U_{ss}(r_{ij}) = \begin{cases} \varepsilon\left[1 - 2\left(\dfrac{\sigma}{r_{ij}}\right)^6\right]^2, & r_{ij} < 2^{1/6}\sigma \\ 0, & r_{ij} > 2^{1/6}\sigma \end{cases} \tag{1}$$

where $r_{ij}$ is a distance between $i$ and $j$ ferroparticles, $\sigma$ is an effective ferroparticle diameter including steric shell, and the energy parameter $\varepsilon$ describes the shell hardness, $U_{ss}(r_{ij} = \sigma) = \varepsilon$. The point dipole–dipole interaction potential is

$$U_d(ij) = -\left[3\frac{(\boldsymbol{m}_i \cdot \boldsymbol{r}_{ij})(\boldsymbol{m}_j \cdot \boldsymbol{r}_{ij})}{r_{ij}^5} - \frac{(\boldsymbol{m}_i \cdot \boldsymbol{m}_j)}{r_{ij}^3}\right], \quad \boldsymbol{r}_{ij} = \boldsymbol{r}_i - \boldsymbol{r}_j \tag{2}$$

The extension of the theory for DHS to DSS systems is done by using an effective hard-sphere diameter mapping. The predictions of the theoretical model are then thoroughly compared to the results of molecular dynamics (MD) simulations. Special emphasis is given to the study of the observed anisotropy of the structure factor in the presence of magnetic fields.

## 2. Theoretical model

The radial distribution function can be written in terms of a virial expansion of the ferroparticle volume concentration $\varphi$ [21]

$$g(r_{12}) = \left\langle \exp\left[-\frac{U_{hs}(r_{12})}{k_BT} - \frac{U_d(12)}{k_BT}\right]\left(1 + \sum_{p=3}^{\infty}\beta_p(12)\varphi^{p-2}\right)\right\rangle_{12} \tag{3}$$

where $U_{hs}$ is the DHS potential. The coefficients $\beta_p(12)$ describe the influence of the other $p-2$ particles on the probability density of the two first ones and are defined by the $p$-particle cluster integrals based on a diagrammatic expansion method [21]. For typical ferroparticle sizes $d \sim 10$ nm, the dipolar coupling constant is close to $\lambda \sim 1$ and therefore Eq. (3) can be written as a power series over $\lambda$:

$$g(r) = \exp\left[-\frac{U_{hs}(r)}{k_BT}\right]\left[\left(1 + \frac{\lambda^2}{3r^6}\right)[1 + h_{hs}(r,\varphi)]\right.$$
$$\left. + \lambda^2\varphi\beta_3^d(r) + \lambda^2\varphi^2\beta_4^d(r) + \lambda^3\varphi\beta_{3*}^d(r)\right] \tag{4}$$

where distances are measured in particle diameter units $r = r_{12}/d$, and $[1 + h_{hs}(r,\varphi)]$ is the hard-sphere radial distribution function, which can be found, for instance, with the help of the Perkus–Yevick approximation [21–23] or the virial expansion [24]. The

$\beta_3^d(r)$ and $\beta_4^d(r)$ contributions were first calculated in Ref. [19]. A previously non-tested three-particle contribution $\lambda^3\varphi\beta_{3*}^d(r)$ which is the next term in importance in the virial expansion has been taken into account in this work. That term can be calculated in a similar way as described in [19] leading to the following expression:

$$\beta_{3*}^d(r) = \begin{cases} 0, & 0 < r < 1 \\ (r^2 - 6)/(18r^2), & 1 \leq r < 2 \\ -\dfrac{16}{9r^6}, & r \geq 2 \end{cases} \tag{5}$$

When an externally magnetic field is applied, it can be proved that the radial distribution function can be written as

$$g(r,\theta) = \exp\left[-\frac{U_{hs}(r)}{k_BT}\right]\left[\left(1 + \lambda L^2(\alpha)\frac{3\cos^2\theta - 1}{r^3} + \frac{\lambda^2}{3r^6}\right)[1 + h_{hs}(r,\varphi)]\right.$$
$$+ \lambda\varphi L^2(\alpha)\frac{3\cos^2\theta - 1}{r^3}\beta_3^{df}(r) + \lambda^2\varphi\beta_3^d(r)$$
$$\left. + \lambda^2\varphi^2\beta_4^d(r) + \lambda^3\varphi\beta_{3*}^d(r)\right], \quad \theta \equiv \theta_{12} \tag{5'}$$

where $L(\alpha) = \coth\alpha - 1/\alpha$ is the squared Langevin function, $\theta$ is the angle between vector $\boldsymbol{r}$ and the direction of the magnetic field. The $\beta_3^{df}(r)$ coefficient is already known from a previous work by Ivanov et al. [25].

Although previous results with the three- and four-contributions calculated by the Ivanov and co-workers [19,25] strictly hold only for DHS, it is very interesting to test if such theory can be or not easily extended to dipolar soft spheres (DSS) using a simple and naive effective hard-sphere diameter $d_e$:

$$d_e = \int_0^{\infty}\left[1 - \exp\left(-\frac{U_{ss}}{k_BT}\right)\right]dr. \tag{6}$$

The effective repulsive energy is set equal to the thermal energy during the simulations, that is $\varepsilon = k_BT$. This yields an effective hard-sphere diameter $d_e$ quite close to $\sigma$: $d_e = 1.016\sigma$.

In order to test such extension of the theory to DSS and get further insight about the dilute low-coupling regime of ferrofluids, equilibrium MD simulations are performed using the simulation package ESPResSo [26]. The simulated systems consist of $N = 1000$ point-dipole particles in a cubic simulation box of side length $L$ where periodic boundary conditions are assumed in all three-directions. The calculation of long-range dipole–dipole interactions has been substantially sped up with the help of a recently developed dipolar P$^3$M algorithm [27].

## 3. Simulation details

Ferrofluids are modeled as systems consisting of $N$ spherical particles of diameter $\sigma$, distributed in a cubic simulation box of side length $L$. Similarly to the theory, we assume particles to be monodisperse, and exhibit a permanent point dipole moment $\boldsymbol{m}$ at its center, which can freely rotate in 3D. The interaction energy between two particles is the sum of the short range interaction equation (1) and the dipolar interaction equation (2). Periodic boundary conditions are assumed along all directions. The long-range dipole–dipole interactions are calculated using a recently developed dipolar P$^3$M algorithm [27]. The use of the dipolar P$^3$M method allows a much faster calculation of the dipolar long-range correlations than the traditional three-dimensional dipolar Ewald summation. The level of accuracy of the algorithm for computing dipolar forces and torques is set to $\delta \sim 10^{-4}$ in reduced units of force $f^* = f\sigma/\varepsilon$ and torque $\tau^* = \tau/\varepsilon$.

Equilibrium molecular dynamics simulations are performed where particles are moved according to the following translational and rotational Langevin equations of motions [28], for particle $i$ the equations are

$$M_i \frac{d\mathbf{v}_i}{dt} = \mathbf{F}_i - \Gamma_T \mathbf{v}_i + \xi_i^T, \tag{7}$$

$$\mathbf{I}_i \cdot \frac{d\boldsymbol{\omega}_i}{dt} = \boldsymbol{\tau}_i + \mathbf{m} \times \mathbf{H} - \Gamma_R \boldsymbol{\omega}_i + \xi_i^R, \tag{8}$$

where $\mathbf{F}_i$, $\boldsymbol{\tau}_i$, and $\mathbf{H}$ are the resulting force, torque and the external magnetic field acting on the particle $i$, respectively. $M_i$ and $\mathbf{I}_i$ are the mass and the inertia tensor of the particle. The symbols $\Gamma_T$ and $\Gamma_R$ stand for the translational and rotational friction constants, respectively. $\xi_i^T$ and $\xi_i^R$ are Gaussian distributed random forces and torques with zero mean, that satisfy the usual fluctuation–dissipation relations. The variables can be given in dimensionless form as length $r^* = r/\sigma$, dipole moment $(m^*)^2 = m^2/(\varepsilon\sigma^3)$, time $t^* = t(\varepsilon/(M\sigma^2))^{(1/2)}$, temperature $T^* = k_B T/\varepsilon$, and external magnetic field $H^* = H(\sigma^3/\varepsilon)^{1/2}$. The simulations are performed at constant temperature $T^* = 1$. Since we are only interested in static observables, the values of the mass, the inertia tensor, as well as friction constants $\Gamma_T$, and $\Gamma_R$ are somewhat at our disposal. The particle mass is chosen to be $M = 1$, and the inertia tensor $\mathbf{I} = \mathbf{1}$, the identity matrix, to ensure isotropic rotations. We adopted $\Gamma_T = 1$ and $\Gamma_R = 3/4$ which are observed in our systems to give a fast relaxation towards the equilibrium. A reduced time step $\Delta t^* \sim 15 \times 10^{-4}$ is used. The runs are started from initial configurations with random particle positions distributed over the simulation volume, and randomly chosen orientations for the dipole moments of the particles. Each system is first equilibrated for a period of $7 \times 10^5$ time steps to ensure that the results are independent of the starting conditions. In order to obtain a proper and almost uncorrelated sampling, measures are taken at intervals of $15 \times 10^3 \Delta t^*$ for another period of $2 \times 10^6$ time steps. The number of particles per system is $N = 1000$ in regular simulations, although several extra runs (up to $N = 10\,000$) have been performed in order to make sure results do not suffer from finite-size effects.

## 4. Results

As in previous numerical studies [29,30], we compute the structure factor as

$$S(\mathbf{q}) = \frac{1}{N} \left\langle \left( \sum_{i=1}^{N} \sin(\mathbf{q} \cdot \mathbf{r}_i) \right)^2 + \left( \sum_{j=1}^{N} \cos(\mathbf{q} \cdot \mathbf{r}_j) \right)^2 \right\rangle, \tag{9}$$

where the wave vectors $\mathbf{q}$ have to be commensurate with the periodic boundary conditions, i.e., $\mathbf{q} \equiv (q_x, q_y, q_z) = (2\pi/L)(l, m, n) \neq (0,0,0)$, where $l$, $m$, and $n$ are integers. For systems without an applied magnetic field, the fluid structure is rotationally invariant, and a spherically averaged structure factor $S(q)$, obtained by averaging over all wave vectors of magnitude $q = |\mathbf{q}|$, is enough to characterize these systems. For the systems with a magnetic field applied along the $z$ direction, $S(\mathbf{q})$ is anisotropic. Nonetheless, it has been shown in previous studies [15,29,31] that it is enough to characterize those systems two different structure factors: one parallel to the magnetic
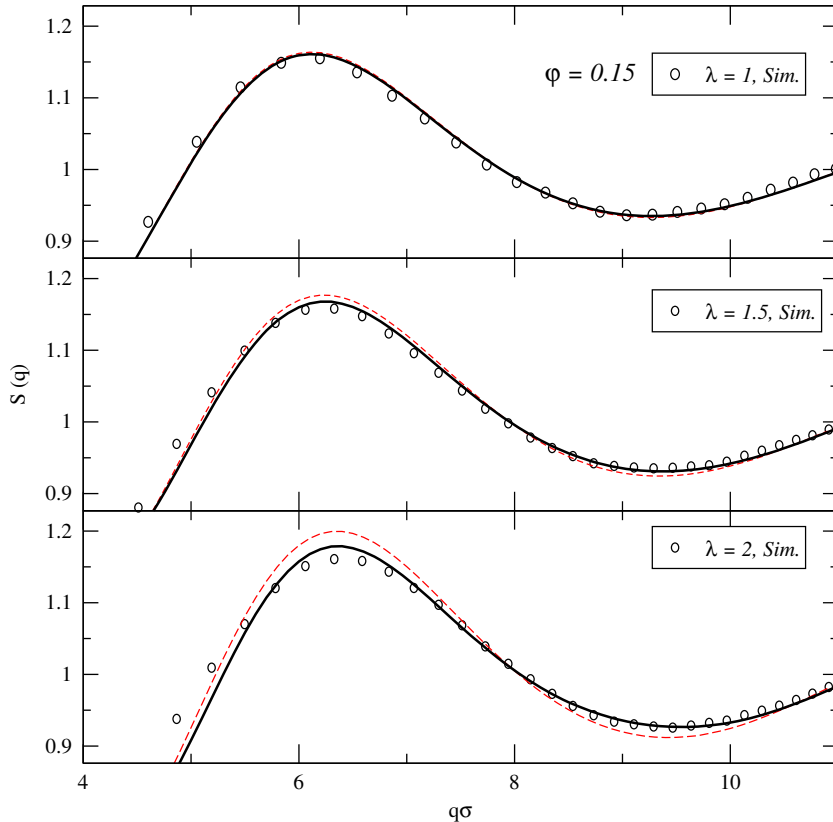


**Fig. 1.** A comparison of the structure factor data obtained at $\varphi = 0.15$ with no applied field, circles stand for simulations, and the solid line for analytical theory results. The value of $\lambda$ changes from top to bottom from $\lambda = 1$ to 1.5, and 2. Solid lines represent theoretical predictions using all terms in Eq. (4) while red dashed lines represent the theoretical predictions when the term $\lambda^3 \varphi \beta_{3*}^d(r)$ is not considered. (For interpretation of the references to color in this figure legend, the reader is referred to the web version of this article.)
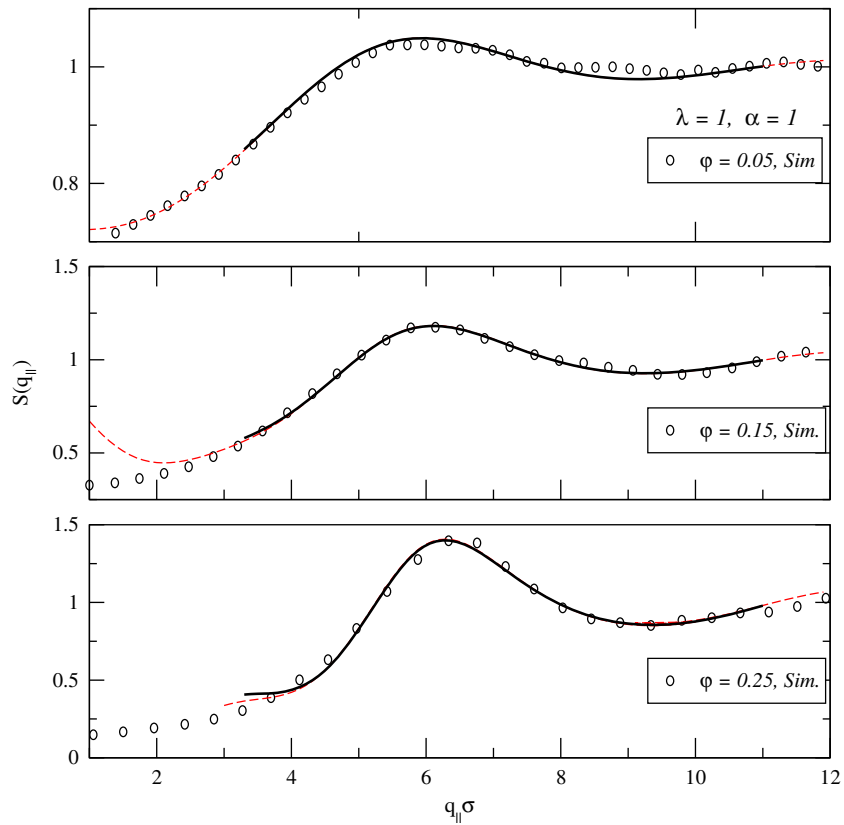
**Fig. 2.** A comparison of the structure factors parallel to the field predicted by the theory and those obtained in numerical simulations is depicted for several volume fractions $\varphi = 0.05, 0.15, 0.25$ at $\lambda = 1$ and Langevin parameter $\alpha = 1$.
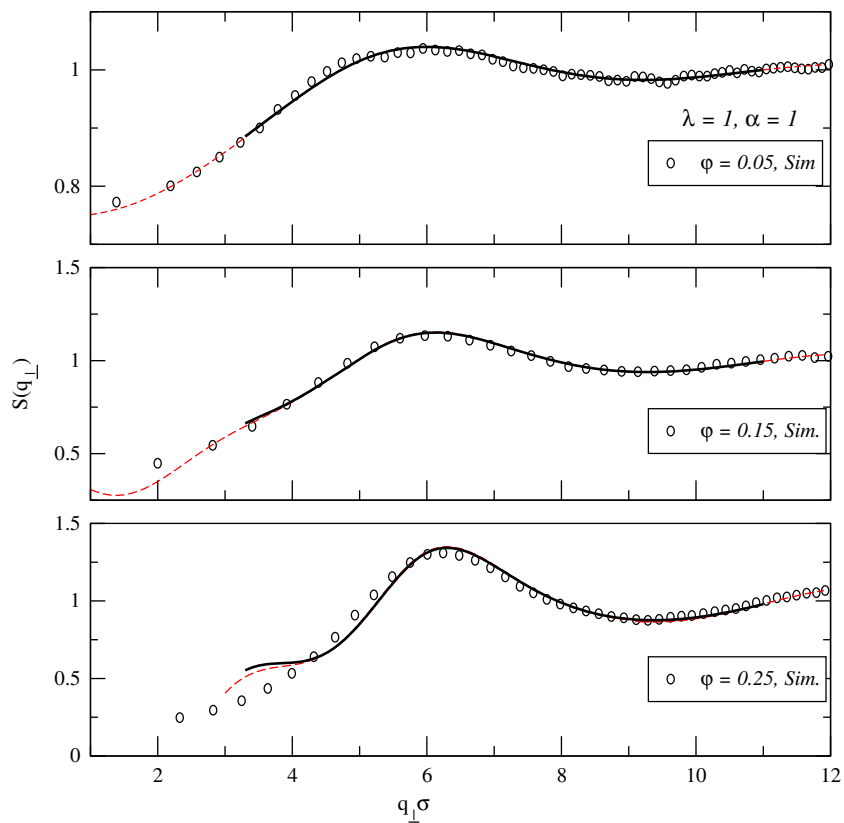


**Fig. 3.** Same as in Fig. 2 but for the component of the structure factor perpendicular to the magnetic field.
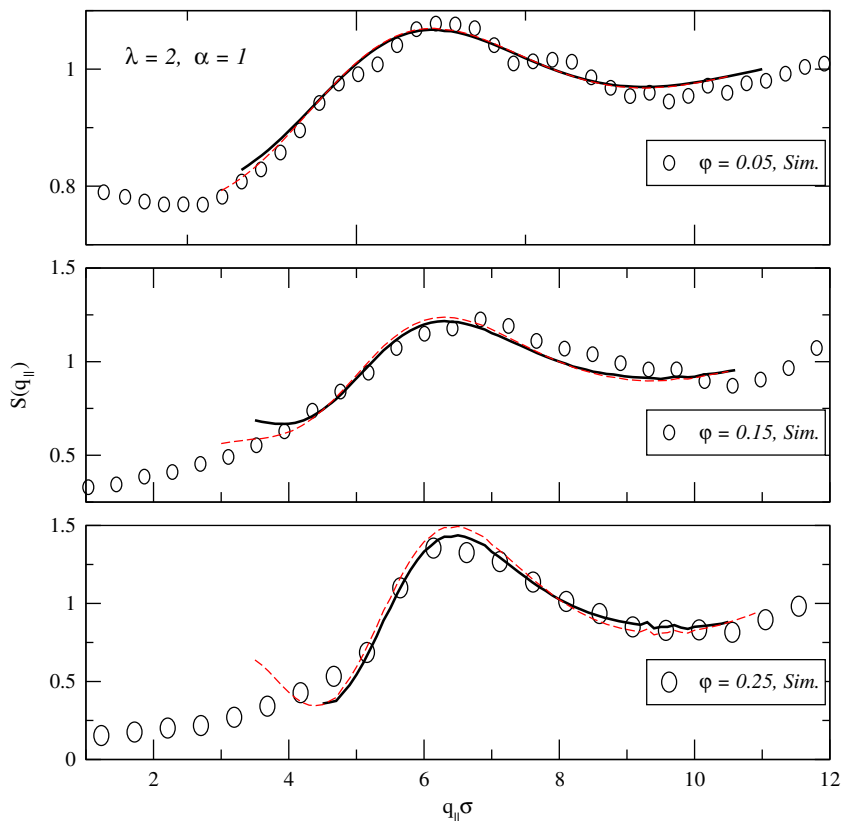
**Fig. 4.** A comparison of the structure factors parallel to the field predicted by the theory and those obtained in numerical simulations is depicted for several volume fractions $\varphi = 0.05, 0.15, 0.25$ at $\lambda = 2$ and Langevin parameter $\alpha = 1$. Solid lines represent theoretical predictions using all terms in Eq. (5′) while red dashed lines represent the theoretical predictions when the term $\lambda^3 \varphi \beta^d_{3*}(r)$ is not considered. (For interpretation of the references to color in this figure legend, the reader is referred to the web version of this article.)
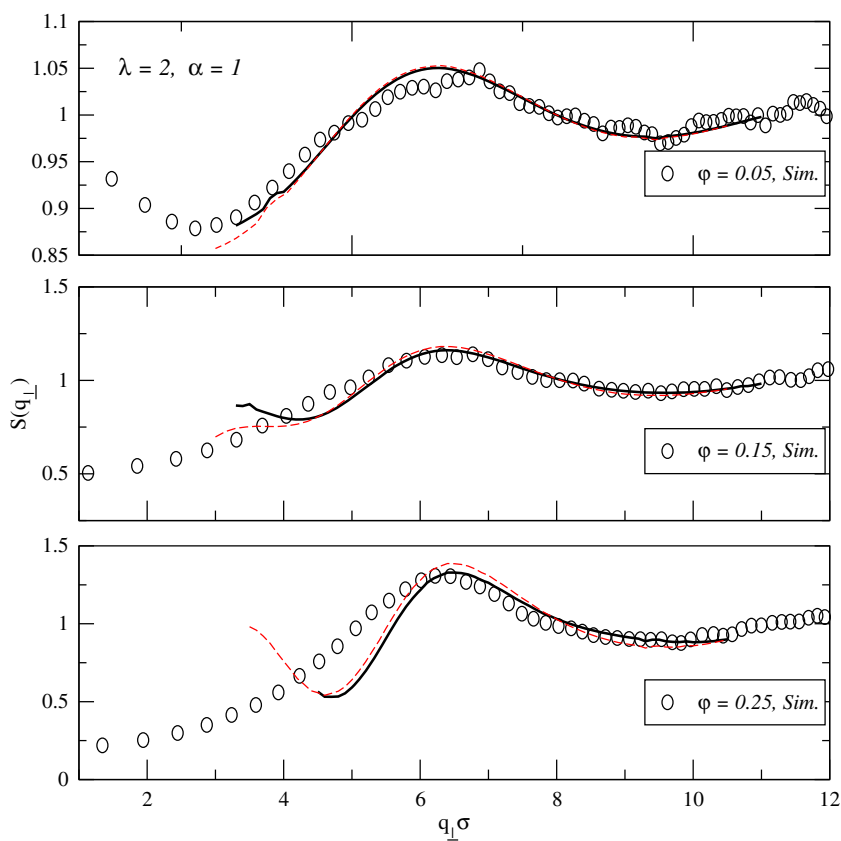


**Fig. 5.** Same as in Fig. 4 but for the component of the structure factor perpendicular to the magnetic field.

field $S(q_\parallel)$ and one perpendicular to the magnetic field $S(q_\perp)$, namely,

$$S(q_\parallel) = \frac{1}{N}\left\langle \left(\sum_{i=1}^{N}\sin(q_\parallel \cdot z_i)\right)^2 + \left(\sum_{j=1}^{N}\cos(q_\parallel \cdot z_j)\right)^2 \right\rangle,$$

$$S(\boldsymbol{q}_\perp) = \frac{1}{N}\left\langle \left(\sum_{i=1}^{N}\sin(\boldsymbol{q}_\perp \cdot \boldsymbol{r}_{xy,i})\right)^2 + \left(\sum_{j=1}^{N}\cos(\boldsymbol{q}_\perp \cdot \boldsymbol{r}_{xy,j})\right)^2 \right\rangle,$$

where $q_\parallel \equiv q_z = (2\pi/L)n$, $\boldsymbol{q}_\perp \equiv (q_x, q_y, 0) = (2\pi/L)(l, m, 0)$, and $\boldsymbol{r}_{xy,i} = (x_i, y_i, 0)$. The rotational symmetry of the system along the z-axis allows us to average the perpendicular structure factor as $S(q_\perp)$ where $q_\perp = |\boldsymbol{q}_\perp| = \sqrt{q_x^2 + q_y^2}$.

Fig. 1 shows for systems without an externally applied magnetic field a comparison of the isotropic structure factor $S(q)$ between theory (lines) and the numerical simulations (open circles) for different values of the dipolar coupling parameter $\lambda = 1, 1.5, 2$ at fixed volume fraction $\varphi = 0.15$. The solid black lines correspond to the theoretical predictions obtained when the new virial term $\lambda^3 \varphi \beta_{3*}^d(r)$ is considered, while the red dashed lines correspond to the results when such term is disregarded. A good agreement between theoretical predictions and simulation results is observed for wave vectors $q\sigma > 3$ in the case of $\lambda = 1$ and $q\sigma > 6$ for $\lambda = 1.5, 2$. The quantitative match increases when the new virial term is taken into account. This fact is specially noticeable for the cases $\lambda > 1$, and as one expects due to the nature of the term $\lambda^3 \varphi \beta_{3*}^d(r)$ increases in importance with $\lambda$. The analysis of the position of the peak maximum positions show that in both theory and simulations, a shift towards higher wave vectors is expected when either $\lambda$ or the volume fraction $\varphi$ are increased. A careful study of the structure factors in the dilute low-coupling regime and the analysis of the underlying microstructure in the systems shows that when dealing with structure factors, one must be very cautious doing an straight identification of the peaks with chains or other types of clusters.

Figs. 2 and 3 show a comparison of the structure factors parallel $S(q_\parallel)$ and perpendicular $S(q_\perp)$ to the magnetic field direction for the case $\lambda = 1$ and $\alpha = 1.0$. Figs. 4 and 5 show $S(q_\parallel)$ and perpendicular $S(q_\perp)$ for the case $\lambda = 2$ and $\alpha = 1.0$. In the presence of a magnetic field, the theoretical predictions obtained when including the new virial term $\lambda^3 \varphi \beta_{3*}^d(r)$ do not bring any substantial improvement in difference to the case $\alpha = 0$. Only at the highest volume fraction systems $\varphi = 0.25$ a slight improvement is observed. The fact that the new correction does not improve substantially the predictions when external magnetic fields are applied can be explained as a consequence of the fact that the new term does not contain a Langevin function dependence. Therefore, this observation implies that by adding high order terms that do not contain Langevin function dependences will not bring any further improvement to the theoretical predictions and therefore are not needed to explain the ferrofluid low-coupling regime. New progress can only be obtained from the derivation of analytical expressions for high order terms having dependencies on the Langevin function. The level of difficulty to derive new contributions of higher order increases substantially and further refinements to the virial expansion will be presented in a forthcoming work.

In Fig. 6 the differences between the averaged density around a particle $\langle \rho(r,z) \rangle$ and the mean bulk density $\rho_0 = N/V$ are presented for increasing external magnetic field strengths $\alpha = 0$ and 5 (figures (a) and (b) respectively) corresponding to the case $\lambda = 2$ and $\varphi = 0.25$. Only results from numerical simulations are presented in this figure. The averaged density around a particle is obtained by calculating the density of particles $\rho(r,z)$ that surrounds a given particle which is set as the origin of coordinates $(r \equiv (x^2+y^2)^{1/2}, z)$ and performing an average of $\rho(r,z)$ over all particles present in the system taken as the origin, and further averaging over all the recorded conformations. In Fig. 7a and b, the
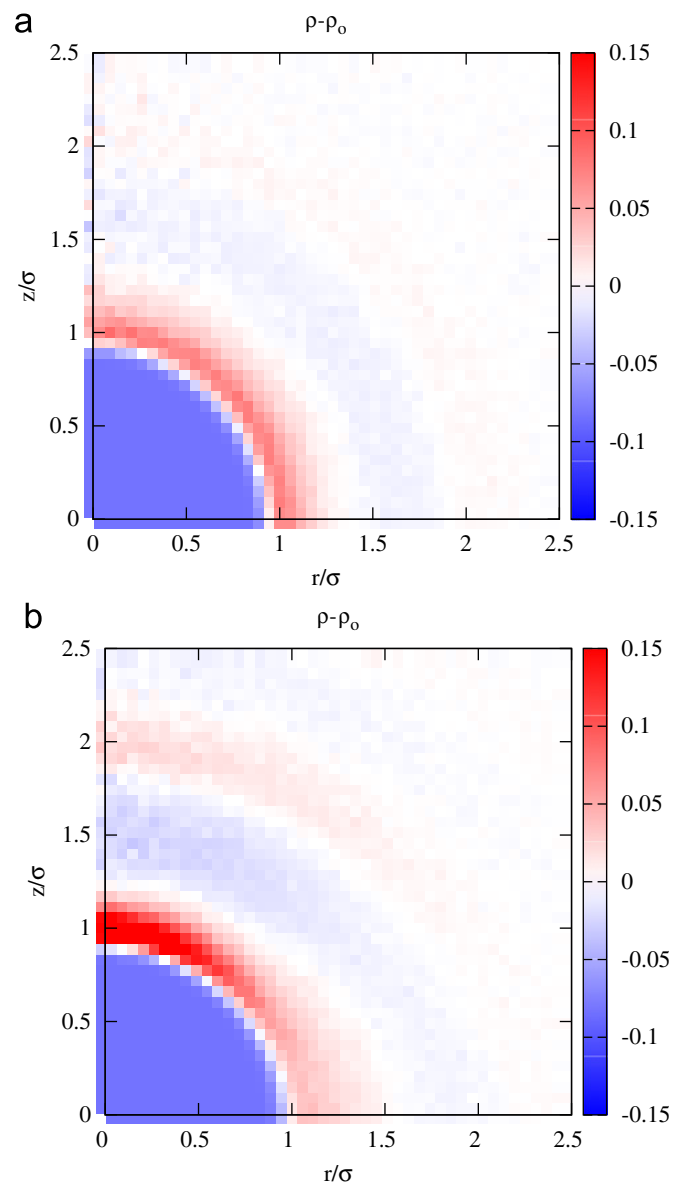


**Fig. 6.** A comparison of the differences between the averaged density around a particle $\langle \rho(r,z) \rangle$ and the mean bulk density $\rho_0 = N/V$ for the case $\lambda = 2$ and $\varphi = 0.25$ for two different intensities of the external magnetic field $\alpha = 0, 5$ ((a) and (b), respectively) are shown. Due to the symmetry of the plot for $+z$ and $-z$, only the upper part is plotted. By definition $r \equiv (x^2+y^2)^{1/2}$. Only simulation data is plotted.

averaged density profile differences at $r=0$ and $z=0$, respectively, are shown for the same case $\lambda = 2$ and $\varphi = 0.25$ than in Fig. 6. It is important to emphasize that the appearance of correlations like those depicted in Figs. 6 and 7 for the case $\lambda = 2$ and $\varphi = 0.25$ are also observed for all $1 < \lambda < 2$ and $\varphi \in [0.05, 0.25]$ cases studied. Our results show clearly that when the magnetic field is applied along the z-direction, despite of the low value of the magnetic interaction between particles $\lambda$ and the density (it also occurs at volume fractions as low as $\varphi = 0.05$) particle correlations exist and are significant in both intensity and range. Thus, when a magnetic field is applied the particles tend to prefer to align along the z-direction with other particles forming kind of denser columnar regions while depleting of particles the surrounding $x–y$ region. This means that although not noticeable by just looking at snapshots of the simulations, particles in average tend to form preferred distributions along the direction of the external magnetic field even in the

a



b
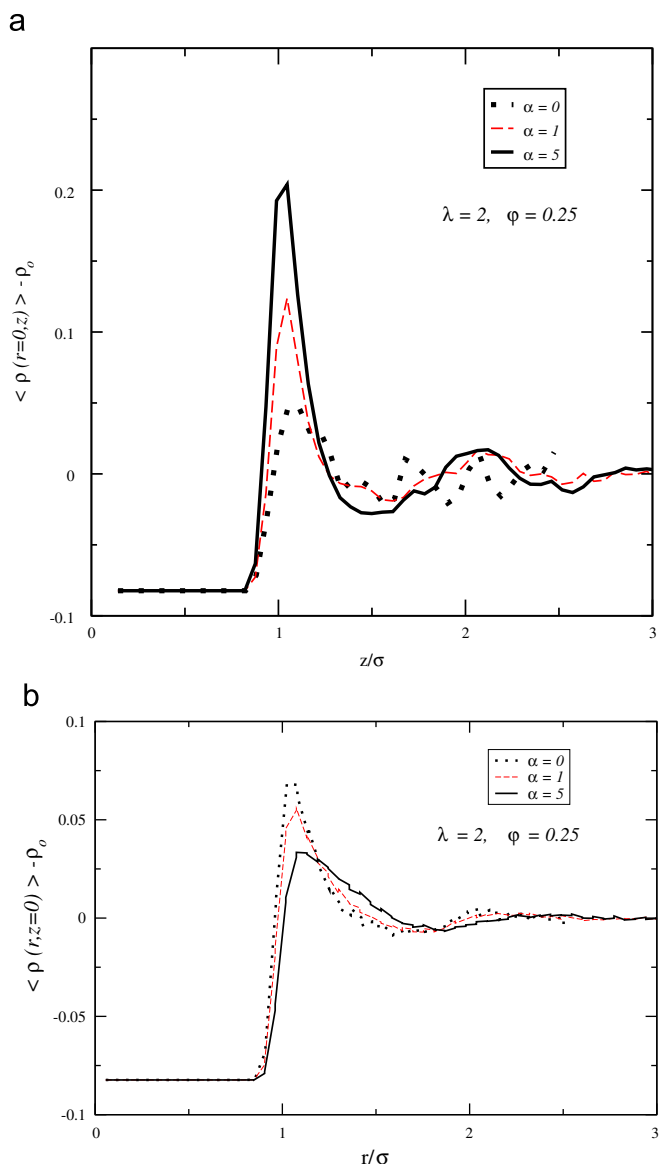


**Fig. 7.** The averaged density profile differences at $r=0$ (a) and $z=0$ (b) obtained from simulations are shown for the case $\lambda = 2$ and $\varphi = 0.25$ for several values of the Langevin parameter $\alpha = 0,1,5$. As in Fig. 6 data supports that when $\alpha$ increases, the particles tend to concentrate along the field direction ($z$ direction) forming column-like structures while in the perpendicular direction $x$–$y$ a depletion phenomena occurs.

case of the dilute low-coupling regime. Remarkably, our observations agree with the recent mean-field predictions of Ciftja [33]: a very simple lattice gas model shows that diluted ferrofluids placed under strong magnetic fields exhibit a second order transition from a homogeneous distribution of particles into a phase with lamellar (stripe) spatial ordering when temperature is reduced below a certain critical temperature that depends on particle concentration. The characterization of the transition found by Ciftja and the study of how these existing correlations inside dilute low-coupling ferrofluids contribute to the rheological and magnetic properties of the fluid will be the object of a forthcoming work.

## 5. Conclusions

In this paper we have tested the suitability of extending a theoretical formalism formerly intended to the case of dipolar hard spheres to the case of dipolar soft spheres. A new term for the virial expansion of the radial distribution function, $\lambda^3 \varphi \beta_{3*}^d(r)$, has been deduced, and a stringent test of its correctness has been done by comparing the results from numerical simulations to the theoretical predictions with and without the new virial term. The study has included both zero and non-zero applied external magnetic field cases.

We have found that despite of the naive and simple approach the extended theory for DSS shows a reasonable agreement for $\lambda \sim 1$ and $\alpha < 5$. The agreement is further improved up to $\lambda \lesssim 2$, at zero field, when the new virial expansion term $\lambda^3 \varphi \beta_{3*}^d(r)$ is considered. Nonetheless, new terms are needed in the case of applied external magnetic fields to get a more quantitative agreement between theory and simulations.

We regard the present theory as complementary to the rod model developed by Pyanzina et al. [32] because it covers the region of low values of the dipolar coupling parameter $\lambda$ where Pyanzina model is not valid due to the pre-assumed existence of stable structures like chains and rings. The combined use of both theories leads to an accurate description of the structure factor for a broad range of dipolar soft-sphere systems [30].

Numerical simulations in addition to assess the quality of the theoretical framework and provide insight about the subjacent microstructure, have revealed that even in the dilute low-coupling regime in the presence of an external magnetic field, strong correlations among particles exist that tend in average to align particles into columnar-like regions aligned along the field. These correlations may arise from a second order transition as noted recently by Ciftja [33] and may have an important contribution to the rheological and magnetic properties of the ferrofluids. We hope the present results will stimulate new studies about the ferrofluid structures and its correlations in the dilute low-coupling regime.

## Acknowledgments

## References

[1] S. Odenbach, Ferrofluids, Magnetically Controllable Fluids and their Applications, in: Lecture Notes in Physics, Springer, New York, 2002.
[2] C.C. Holm, J.J. Weis, Curr. Opin. Colloid Interface Sci. 10 (2005) 133.
[3] S. Odenbach, Coll. Surf. A: Physicochem. Eng. Aspects 217 (2003) 171.
[4] M.I. Shliomis, Sov. Phys. Usp. 153 (1974) 17.
[5] A. Tsebers, Magnetohydrodynamics (N.Y.) 18 (1982) 345.
[6] A.F. Pshenichnikov, V.V. Mekhonoshin, A.V. Lebedev, J. Magn. Magn. Mater. 161 (1996) 94.
[7] M.S. Wertheim, J. Chem. Phys. 55 (1971) 4291.
[8] K.I. Morozov, Bull. Acad. Sci. USSR, Phys. Ser. (Engl. Transl.) 51 (1987) 32.
[9] K.I. Morozov, A.V. Lebedev, J. Magn. Magn. Mater. 85 (1989) 51.
[10] G.S. Rusbroo, G. Stell, J.S. Hoye, Mol. Phys. 26 (1973) 1199.
[11] J. Wagner, B. Fischer, T. Autenrieth, J. Chem. Phys. 124 (2006) 114901.
[12] I. Szalai, S. Dietrich, J. Phys. Condens. Matter 20 (2008) 204122.
[13] Y.A. Buyevich, A.O. Ivanov, Physica A 190 (1992) 276.
[14] A.O. Ivanov, Magnetohydrodynamics (N.Y.) 28 (1992) 39.
[15] F. Gazeau, E. Dubois, J.C. Bacri, F. Boue, A. Cebers, R. Perzynski, Phys. Rev. E 65 (2002) 031403.
[16] J. Wagner, B. Fischer, T. Autenrieth, R. Hempelmann, J. Phys. Condens. Matter 18 (2006) S2697.
[17] A. Wiedenmann, M. Kammel, A. Heinemann, U. Keiderking, J. Phys. Condens. Matter 18 (2006) S2713.
[18] L.M. Pop, S. Odenbach, J. Phys. Condens. Matter 18 (2006) S2785.
[19] E. Elfimova, A. Ivanov, Magnetohydrodynamics 44 (2008) 39.
[20] J.D. Weeks, D. Chandler, H.C. Andersen, J. Chem. Phys. 54 (1971) 5237.
[21] R. Balescu, Equilibrium and Nonequilibrium Statistical Mechanics, Wiley, New York, 1975.
[22] M.S. Wertheim, Phys. Rev. Lett. 10 (1963) 321.
[23] J. Chaang, S.I. Sandler, Mol. Phys. 735 (1994) 81.
[24] B.R.A. Nijboer, L. Van Hove, Phys. Rev. 85 (1952) 777.

[25] A.O. Ivanov, O.B. Kuznetsova, Phys. Rev. E 64 (2001) 041405.

[26] H.J. Limbach, A. Arnold, B.A. Mann, C. Holm, Comput. Phys. Commun. 174 (2006) 704.

[27] J.J. Cerdà, V. Ballenegger, O. Lenz, C. Holm, J. Chem. Phys. 129 (2008) 234104.

[28] M.P. Allen, D.J. Tildesley, Computer Simulation of Liquids, Clarendon Press, Oxford, 1987.

[29] J.P. Huang, Z.W. Wang, C. Holm, Phys. Rev. E 71 (2005) 061203.

[30] J.J. Cerdà, E. Elfimova, V. Ballenegger, E. Krutikova, A. Ivanov, C. Holm, Phys. Rev. E 81 (2010) 011501.

[31] G. Mériguet, M. Jardat, P. Turq, J. Chem. Phys. 121 (2004) 6078.

[32] E. Pyanzina, S.S. Kantorovich, J.J. Cerdà, A. Ivanov, C. Holm, Mol. Phys. 107 (2009) 571.

[33] O. Ciftja, Solid State Commun. 149 (2009) 532.